

Heavy-Fermion Superconductivity in CeAg₂Si₂ –Interplay of Spin and Valence Fluctuations–

Gernot W. Scheerer* and Didier Jaccard
DQMP - University of Geneva, 1211 Geneva 4, Switzerland.

Zhi Ren

Institute for Natural Sciences, Westlake Institute for Advanced Study, Hangzhou, P. R. China.

G erard Lapertot

SPSMS, UMR-E 9001, CEA-INAC/UJF-Grenoble 1, 38054 Grenoble, France.

Gaston Garbarino

European Synchrotron Radiation Facility, 38043 Grenoble Cedex 9, France.

(Dated: November 6, 2018)

We present the pressure-temperature phase diagram of the antiferromagnet CeAg₂Si₂ established via resistivity and calorimetry measurements under quasi-hydrostatic conditions up to 22.5 GPa. With increasing pressure, the N eel temperature [$T_N(p=0) = 8.6$ K] slowly increases up to $T_N = 13.4$ K at 9.4 GPa and then vanishes abruptly at the magnetic critical pressure $p_c \sim 13$ GPa. For the first time, heavy fermion superconductivity is observed in CeAg₂Si₂. Superconductivity emerges at ~ 11 GPa and persists over roughly 10 GPa. Partial- and bulk-transition temperatures are highest at $p = 16$ GPa, with a maximal $T_{c,\text{bulk}} = 1.25$ K. In the pressure region of superconductivity, Kondo and crystal-field splitting energies become comparable and resistivity exhibits clear signatures of a Ce-ion valence crossover. The crossover line is located at a rapid collapse in resistivity as function of pressure and extrapolates to a valence transition critical endpoint at critical pressure and temperature of $p_{cr} \sim 17$ GPa and $T_{cr} \sim -13$ K, respectively. Both critical spin and valence fluctuations may build up superconductivity in CeAg₂Si₂.

Keywords: CeAg₂Si₂, heavy-fermion superconductivity, pressure-temperature phase diagram, critical valence fluctuation, valence crossover

I. INTRODUCTION

Superconductivity (SC) in heavy fermion (HF) systems is thought to be mediated by critical fluctuations [1–6], while there is no general consensus about the exact nature of the fluctuations. Especially in the case of SC in the compounds CeCu₂Si₂ [7–9], CeCu₂Ge₂ [10], and CeCu₂(Si_{1-x}Ge_x)₂ [11], there are two dominant scenarios. One considers that the low-pressure SC is mediated by the critical spin fluctuations resulting from the collapse of an antiferromagnetic (AF) phase at p_c [6, 12]. The other, mainly defended by Prof. K. Miyake and coworkers, is that critical valence fluctuations (CVF) of a valence crossover (VCO) at p_v play the dominant role for the high-pressure SC, when T_c is optimal close to p_v [13–15]. Another noteworthy case is the most recently discovered HF superconductor CeAu₂Si₂ [16]. Its phase diagram is markedly different from all previous cases and –showing also clear features of the CVF picture [16–19] – revives the debate about the current understanding of superconductivity and magnetism in heavy fermion sys-

tems. Naturally, the next step is to the search for SC in the isoelectronic and isostructural compound CeAg₂Si₂.

CeAg₂Si₂ has a tetragonal ThCr₂Si₂ structure with the space group $I4/mmm$ (D_{4h}^{17}) [20]. The Ce ion is nearly trivalent and its $4f$ $J = \frac{5}{2}$ multiplet is split into 3 doublets by the crystal electric field (CEF) with the first and second excited doublets at 8.8 and 18.0 meV, respectively [21]. The system exhibits weak Kondo-lattice resistivity and thermopower behavior [22] and the estimated Kondo temperature is $T_K = 1.7$ K [21]. CeAg₂Si₂ undergoes an AF transition at the N eel temperature $T_N = 8.6$ K [23–25]. The magnetic order is either a spin density wave or a square-wave structure both with spins aligned along the a -axis [20]. A previous pressure study (limited to 1.5 GPa) indicates that T_N increases linearly with increasing pressure [24].

We scanned the pressure-temperature (p - T) phase diagram of high quality CeAg₂Si₂ crystals via resistivity and ac heat capacity measurements, and discovered a large dome of SC centered around $p = 16$ GPa with a maximum critical temperature of $T_c = 1.25$ K. With increasing pressure, T_N increases up to a maximum $T_N = 13.4$ K at $p \sim 9.4$ GPa, then decreases and vanishes rapidly at the magnetic critical pressure $p_c \sim 13$ GPa. SC emerges close to p_c and persists over roughly 10 GPa. An effective mass of $\sim 190\times$ the free electron mass is deduced from the large initial slope of the upper critical field, indicating that SC is build up by heavy quasiparticles. Properties of the normal-state resistivity (residual resistivity ρ_0 , power-law coefficient A and exponent n) are extracted

* gernot.scheerer@unige.ch

under an applied magnetic field. Strongly enhanced scattering rates occur around p_c , indicating enhanced spin fluctuations. A drastic collapse of the coefficient A in the pressure region of SC is ascribed to the rapid delocalization of the Ce 4f electrons. Resistivity exhibits a scaling behavior suggesting the presence of a VCO, similar to that in CeCu_2Si_2 [15] and CeAu_2Si_2 [16]. The VCO arises from the critical end point (CEP) of an underlying, putative first-order-valence transition at negative temperature. The resulting critical pressure and temperature of the CEP are $p_{\text{cr}} \sim 17$ GPa and $T_{\text{cr}} \sim -13$ K, respectively. We discuss the possibility that SC in CeAg_2Si_2 is driven by critical valence fluctuations.

II. EXPERIMENT

The experiment was done with CeAg_2Si_2 single crystals (see Ref. [16] for details on crystal-growth method). The data were obtained in two different Bridgman-type pressure cells, one with sintered-diamond anvils ($p^{\text{max}} = 22.5$ GPa) and the other with tungsten-carbide anvils ($p^{\text{max}} = 10$ GPa). Both cells were closed with a pyrophyllite gasket and filled with steatite as soft-solid pressure medium. Temperature and magnetic field were controlled by a standard dilution fridge equipped with a superconducting magnet coil ($\mu H^{\text{max}} = 8.5$ T). Rod shaped samples were cut from the same batch with a slow-cut diamond saw ($\approx 20 \times 50 \times 600 \mu\text{m}^3$, sample length along the basal plane). The samples residual resistivity and RRR at ambient pressure are $5.5 \mu\Omega\cdot\text{cm}$ and 4.55 respectively. The magnetic field was applied along the c -axis. The dc resistivity was measured with linear four-point contacts and the ac heat capacity via a system of local heater and thermocouple (see Refs. [9, 16, 26] for technical details). Heat capacity was measured in the tungsten-carbide anvil cell for pressures $2 \leq p \leq 10$ GPa. Pressure was determined from the resistive superconducting transition temperature of a lead strip. The pressure gradient along the sample estimated from the transition width was ≈ 0.5 GPa at low pressure and increased progressively up to ≈ 1.4 GPa at maximum pressure.

Additionally, we studied the compressibility of CeAg_2Si_2 at ambient temperature via X-ray scattering (GSAS and CrysAlis at ESRF, data not shown here). An anomaly is found in the compressibility at ~ 20 GPa, which may be related to a valence instability.

III. RESULTS

Figure 1 presents the electronic resistivity $\rho - \rho_{\text{ph}}$ versus temperature T of CeAg_2Si_2 measured at pressures p up to 22.5 GPa, where ρ_{ph} is the pressure-independent phonon term derived from LaPd_2Si_2 [27]. Overall temperature and pressure dependences of resistivity are typical for a Ce-based Kondo lattice [10]. Characteristic are the anomaly at the Néel temperature T_N , the two broad

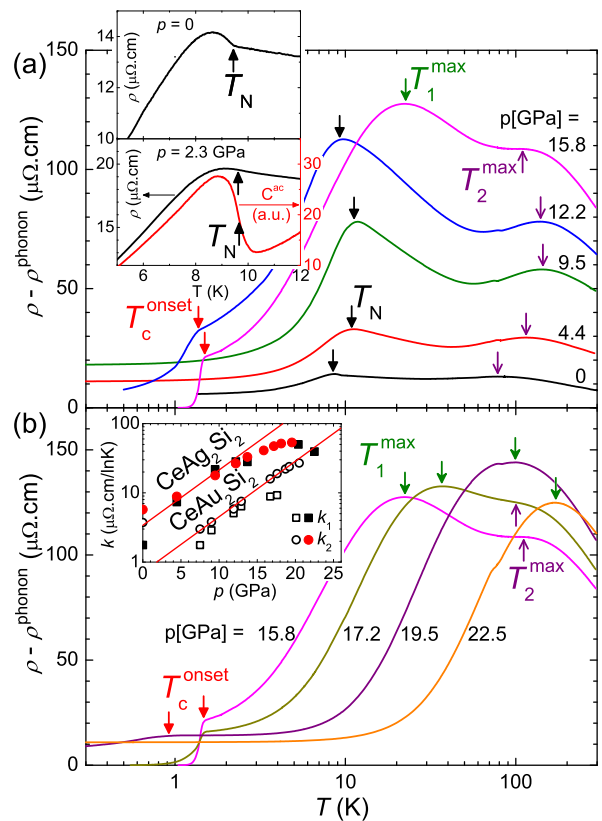


FIG. 1. (a,b) Resistivity $\rho - \rho_{\text{ph}}$ versus temperature T (log-scale) of CeAg_2Si_2 at selected pressures, where ρ_{ph} is the phonon-term derived from LaPd_2Si_2 . Arrows indicate the Néel temperature T_N , onset temperature T_c^{onset} of SC, and the characteristic temperatures T_1^{max} and T_2^{max} (see text). Bulk SC occurs at the $\rho = 0$ criteria. Inset of (a): $\rho(T)$ at zero pressure and $\rho(T)$ and $C^{\text{ac}}(T)$ at 2.3 GPa around T_N . Inset of (b): $-\ln T$ slopes k_1 and k_2 extracted via linear fits on $\rho(\ln T)$ above T_1^{max} and T_2^{max} , respectively. k_1 and k_2 of CeAu_2Si_2 from Ref. [18] is added for comparison. The solid lines are a guide to the eyes.

maxima at T_1^{max} and T_2^{max} , and the resistivity drop at the superconducting transition temperature T_c . The amplitude of ρ at T_1^{max} increases with increasing pressure due to the increasing c -f coupling J_K .

The signature of the AF transition in ρ at T_N is sharp at zero pressure but gets more and more blurred with increasing pressure [see inset of Fig. 1(a)]. However, the pressure induced increase of T_N is clearly established by the anomaly in the ac heat capacity C^{ac} [see inset of Fig. 1(a)]. Missing C^{ac} data above 10 GPa, the rapid vanishing of T_N between 12.2 and 13.7 GPa is established by resistivity only. Below T_N , ρ drops rapidly with decreasing temperature and is governed by electron-magnon scattering. The maxima at T_1^{max} and T_2^{max} are due to the crossover from coherent to incoherent Kondo scattering on the Ce 4f-ground state and excited CEF levels, respectively [28]. At low pressure, $T_1^{\text{max}} < T_N$ and the resistivity maximum at T_1^{max} is cut by the onset

of coherent electron-magnon scattering. T_1^{\max} increases rapidly with increasing pressure, while T_2^{\max} is rather p -independent. The resistivity maxima at T_1^{\max} and T_2^{\max} merge at ~ 19 GPa, i.e. near the pressure of optimal SC [see also Fig. 2(a)], which is actually a hallmark of Ce-based HF superconductors [10, 16, 29–33] and indicates that Kondo and CEF splitting energies become comparable in this pressure region [34]. Above ~ 19 GPa, a single maximum remains due to the dominating contribution of T_1^{\max} . In the incoherent scattering regimes above T_1^{\max} and T_2^{\max} , the resistivity decreases as $-k_i \ln T$ with the logarithmic slopes k_1 and k_2 , respectively. The pressure dependence of k_1 and k_2 [inset of Fig. 1(b)] is similar to that found in CeAu₂Si₂ [18] and points to a constant ratio k_2/k_1 as expected from theory [28]. However, one expects $k_1 < k_2$, which hints to an underestimation of the phonon contribution ρ_{ph} . The saturation of k_1 and k_2 at high pressures is an artifact due to the convergence of T_1^{\max} and T_2^{\max} and the limited temperature scale, respectively. The significant increase of the $-\ln T$ slopes indicates the pressure induced enhancement of the Kondo temperature T_K by roughly one order of magnitude over the investigated pressure range [28].

Partial SC sets in at T_c^{onset} and the transition completes with $\rho = 0$, where bulk SC is presumably established [35]. Optimal SC with $T_c^{\text{bulk}} = 1.25$ K and $T_c^{\text{onset}} = 1.57$ K occurs at $p = 15.8$ GPa. At the same pressure, scans of the resistive transition under magnetic field yield the SC upper critical field $H_{c2} = 5.75$ T and the initial slope $H'_{c2} = dH_{c2}/dT|_{T \rightarrow T_c} \approx -11$ T/K for the $\rho = 0$ criteria. The onset criteria yields $H_{c2}^{\text{onset}} \approx 7.5$ T and $H'_{c2} \approx 25$ T/K. The H'_{c2} value gives a clean-limit effective mass of $m^* \sim 190 m_0$ [36], where m_0 is the free-electron mass. Thus, SC in CeAg₂Si₂ is build up by HF quasiparticles.

Figure 2(a) presents the p - T phase diagram of CeAg₂Si₂ resulting from our resistivity and heat capacity measurements. Again, the overall appearance is the one of a Ce-based HF system. A low-pressure AF phase vanishes at the critical pressure p_c resulting in a paramagnetic ground state above p_c and an intermediate valence regime is reached at still higher pressure. All is controlled by the increasing Kondo scale T_K , which is initially of the order of 2 K and increases rapidly by more than one order of magnitude, as indicated by the characteristic temperature T_1^{\max} .

Peculiarity in CeAg₂Si₂ are the details of the magnetic and superconducting phases. The Néel temperature T_N ($= 8.6$ K at $p = 0$) increases with increasing pressure up to a maximum $T_N = 13.4$ K at $p \sim 9.4$ GPa and suddenly vanishes at p_c between 12.2 and 13.7 GPa. Note that T_N drops from about 10 K to zero over a narrow pressure interval of less than 1.5 GPa. Considering a p gradient along the sample of ~ 1 GPa, the collapse is much more rapid than usually observed in Ce-based HF compounds.

Partial SC emerges at around 11 GP just before the collapse of the AF order at p_c and spans over a remarkably wide pressure range of roughly 10 GPa. Bulk

SC ($\rho = 0$) emerges around 13.5 GPa and vanishes around 17.5 GPa, which still is a broad pressure range of ~ 4 GPa. The dome of SC culminates at $p = 15.8$ GPa with $T_c^{\text{bulk}} = 1.25$ K and $T_c^{\text{onset}} = 1.57$ K. One can expect to find a higher T_c and a much larger area of bulk SC in samples of better quality [17]. The overlap of partial SC and AF phase of roughly 2 GPa is small compared to the total area of SC and optimal bulk SC occurs roughly 3 GPa above the AF collapse at p_c . For comparison, there is a similar small overlap in CeCu₂(Si/Ge)₂ [10], where the maximum T_c occurs at $p \sim p_c + 4.5$ GPa, while CeAu₂Si₂ [16] exhibits is a huge overlap (~ 12 GPa) of SC with the magnetic phase, where latter vanishes just at the maximum T_c . Common features are the relatively high maximal T_c (≥ 1.25 K) and the very broad domes of SC ($\Delta p > 7$ GPa), which distinguish the CeCu₂Si₂-HF family.

Let us now discuss the properties of the normal-state resistivity measured under a magnetic field $H = 8$ T $> H_{c2}^{\text{onset}}$. At lowest temperatures ($T < \frac{1}{10}T_N$, $T < \frac{1}{10}T_1^{\max}$), the resistivity $\rho(T)$ is well described by a simple power law $\rho = \rho_0 + A \cdot T^n$. Figure 2 presents the pressure dependences of the residual resistivity ρ_0 , the coefficient A , and the exponent n . Both ρ_0 and A increase with increasing pressure by a factor of ≈ 5 and ≈ 55 , respectively, up to a maximum at $p = 13.7$ GPa close to the magnetic p_c . Above 13.7 GPa, ρ_0 decreases by a factor of 2 and stabilizes on a shoulder at $p \sim 19$ GPa. The coefficient A decreases by more than 2 orders of magnitude from 13.7 GPa up to $p^{\text{max}} = 22.5$ GPa. The peak in ρ_0 around p_c is ascribed to enhanced impurity scattering presumably due to enhanced spin [37] or charge [38] fluctuations, and the shoulder around 19 GPa may be due to a VCO [39]. The 55 fold increase in A may be attributed to two different phenomena, which are the recovering of paramagnetic c-f Kondo scattering through the collapse of magnetic order [19] and the enhancement of the quasiparticles effective mass $m^* \propto \sqrt{A}$ due to critical fluctuations [40]. The drastic collapse in A above 13.5 GPa results from the rapid delocalization of the Ce 4f electrons, when pressure drives the system from trivalent to intermediate valence regime [9, 15]. Identical observations in CeCu₂Si₂ [9, 41], CeCu₂Ge₂ [10], and CeAu₂Si₂ [16, 19] are attributed to a pressure induced VCO at p_v close to the pressure of optimal SC.

From residual electron-magnon scattering in the AF state ($T \ll T_N$), one expects a Fermi-liquid like $n \approx 2$, which is the case at zero pressure and close to p_c . At intermediate pressures ~ 5 GPa, values of n smaller than 2 may be due to a magnetic structure effect, as observed in the parent compounds [19, 42, 43]. In the paramagnetic state above p_c , n is scattered between $\sim 1.6 - 2$ with a minimum at 19.5 GPa.

The existence of the putative VCO can be corroborated by a resistivity scaling analysis, which was first elaborated by Seyfarth *et al.* [15] on data from CeCu₂Si₂. Before applying the same method on the present ρ data, we recall that theory based on the extension of the

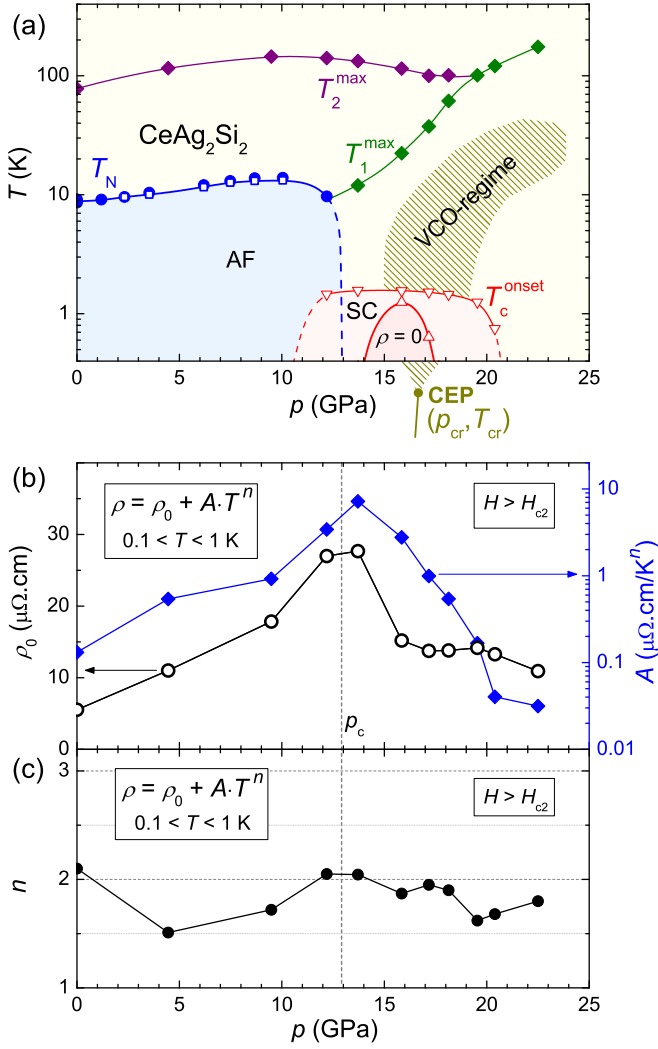


FIG. 2. (a) p - T phase diagram of CeAg_2Si_2 resulting from resistivity and ac heat capacity measurements in quasi-hydrostatic conditions. T_1^{max} , T_2^{max} , and T_c are based on resistivity. T_N is based on resistivity (full circles) and ac heat capacity (empty squares). (b) and (c) Pressure dependences of the fitting parameters of the power law $\rho(T) = \rho_0 + A \cdot T^n$ extracted from the the normal-state resistivity ($H = 8$ T $> H_{c2}^{\text{onset}}$) for $0.1 < T < 1$ K.

periodic Andersen model by the supplementary term $U_{\text{fc}} \sum_{i=1}^N n_i^f n_i^c$, where U_{fc} is the Coulomb repulsion between f and conduction electrons, predicts a pressure induced VCO for small values of U_{fc} and predicts CVF mediated Cooper pairing in proximity of the VCO [44, 45]. In CeCu_2Si_2 , such a VCO with a critical end point (CEP) at slightly negative critical temperature $T_{\text{cr}} \sim -8$ K was found at $p_v \sim 4$ GPa, i.e., just at the pressure of optimal SC [15].

The scaling analysis [15] starts with plotting the resistivity isotherms $\rho^* = \rho - \rho_0$ at different temperatures, as shown in Fig. 3(a). After a maximum at $p \sim 15$ GPa, ρ^* decreases by one to two orders of magnitude with increasing pressure. As the collapse of the A coefficient in the

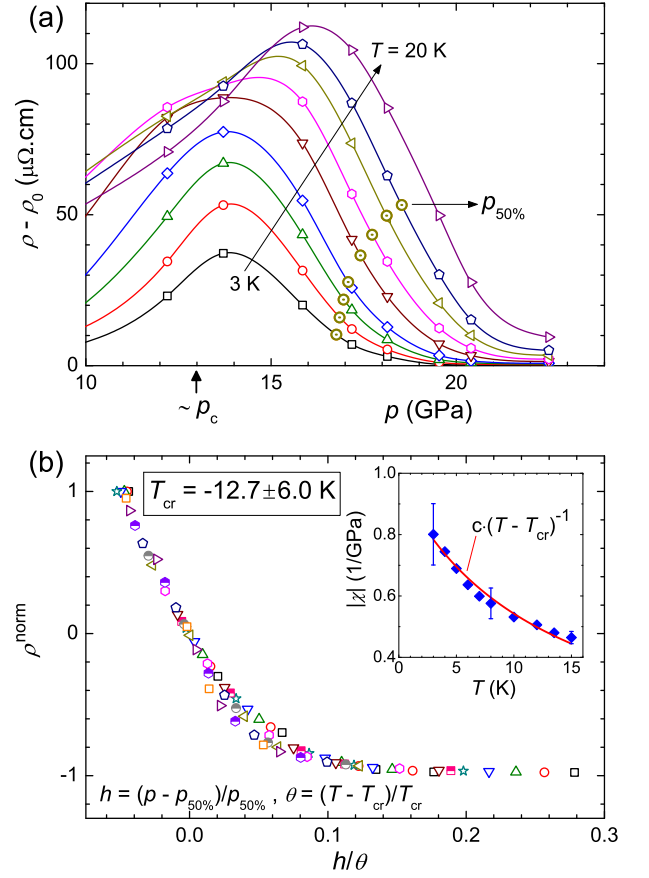


FIG. 3. (a) Isotherms of $\rho - \rho_0$ at temperatures between 3 and 20 K. The pressure $p_{50\%}$ is defined at the 50% drop of $\rho - \rho_0$ compared to an initial value at $p_{\text{in}} = 15.85$ GPa. The spline lines are guides to the eyes. (b) Normalized resistivity isotherms ρ^{norm} versus the generalized distance from the CEP h/θ (see text for details) for temperatures from 3 to 22.5 K. Inset: Temperature dependence of the slope χ (see text for details). The value $T_{\text{cr}} = -12.7$ K is extracted via a fit with $\chi = c \cdot (T - T_{\text{cr}})^{-1}$ (red line). The estimated error on T_{cr} is ± 6.0 K.

same p region, the decrease in ρ^* is a direct consequence of the rapid delocalization of the f electrons through the VCO. The absence of any discontinuity in $\rho^*(p)$ down to lowest temperatures confirms the crossover nature of the valence instability. At lowest temperature the drop of $\rho^*(p)$ is steepest at ≈ 16 GPa, indicating that the center of the VCO occurs close to optimal SC [see Fig. 2(a)].

Following [15], we define a normalized resistivity $\rho^{\text{norm}}(p) = \frac{\rho^*(p) - \rho^*(p_{50\%})}{\rho^*(p_{50\%})}$, where $p_{50\%}$ is defined by the 50% drop of $\rho^*(p)$ compared to an initial value at $p_{\text{in}} = 15.8$ GPa (fixed for all temperatures). p_{in} marks the onset of the decrease of $\rho^*(p)$ at intermediate temperatures and $p_{\text{in}} > p_c$. The normalization is necessary to separate the effect of the f electron delocalization from the temperature dependence. The steepness of the resistivity collapse defined as $\chi = |d\rho^{\text{norm}}/dp|_{p_{50\%}}$ diverges when $T \rightarrow T_{\text{cr}}$ [inset of Fig. 3(b)]. A fit with the well

established temperature dependence $\chi \propto (T - T_{\text{cr}})^{-1}$ [15–17] yields $T_{\text{cr}} = -12.7 \pm 6.0$ K. Note that the analysis is limited to $T \leq 15$ K, which corresponds to a small fraction to of the first CEF-splitting energy. Now, one can calculate the general distance h/θ from the CEP, where $h = (p - p_{50\%})/p_{50\%}$ and $\theta = (T - T_{\text{cr}})/|T_{\text{cr}}|$. Figure 3(b) shows that all curves ρ^{norm} versus h/θ collapse on a single scaling function. The resistivity behavior of CeAg₂Si₂ clearly indicates a pressure-induced VCO, which arises from the CEP of an underlying first-order-valence transition at critical negative temperature $T_{\text{cr}} \sim -13$ K and at critical pressure p_{cr} of roughly 17 GPa.

IV. DISCUSSION

In CeAg₂Si₂ and in its isovalent and isostructural parent compounds CeCu₂Si₂, CeCu₂Ge₂ and CeAu₂Si₂ resistivity behaves very similar, and especially the merge of T_1^{max} and T_2^{max} , the rapid collapse of A and ρ^* as function of pressure, and the resistivity-scaling behavior are recurring signatures ascribed to a valence instability [5, 9, 10, 15, 16, 18]. Following the scaling analysis of Ref. [15], systematically, a VCO is found at pressures close to the pressure of optimal SC [15, 16]. Therefore, one has to consider valence fluctuations as plausible superconducting mechanism [44, 45]. In such a scenario, a less higher $T_c = 1.25$ K in CeAg₂Si₂ compared to $T_c \approx 2.5$ K in CeCu₂Si₂ and CeAu₂Si₂ may be due to a moderately high residual scattering [46] and weaker valence fluctuations at finite temperatures from a more negative CEP [44]. Later may also explain that CeAg₂Si₂ exhibits only a minimum $n = 1.6$ and a weak shoulder in ρ_0 in the VCO regime, while CVF theory predicts non-fermi liquid behavior with $n = 1$ [9] and a peak in ρ_0 around p_v [39] as observed in CeCu₂Si₂ [9].

Spin fluctuations are believed to be the canonical superconducting mechanism near a magnetic quantum critical point (QCP) in Ce-based HF compounds [4]. Indeed, SC emerges close to the collapse of AF order in CeAg₂Si₂. However let us mention some points, which are not in favor of the spin fluctuation scenario.

(i) The rapid collapse of magnetism and a power law exponent $n \approx 2$ around p_c may be interpret as the absence of a magnetic QCP. It has been shown theoretically [14, 47] that, in the case of weak c-f hybridization

and thus a hypothetical magnetic QCP at pressure p_{QCP} higher than p_{cr} , it is possible that the VCO drives a first-order collapse of magnetism at p_c ($< p_{\text{cr}} < p_{\text{QCP}}$). In this case, the peaks in ρ_0 and A at ~ 13 GPa may be due to enhanced charge fluctuations due to competition between inter-site and Kondo-Yosida singlets, when $T_K \sim T_1^{\text{max}}$ becomes comparable to T_N [38], which is indeed observed [see Fig. 2(a)].

(ii) When spin fluctuations are believed to mediate SC, optimal SC occurs close to the magnetic QCP and T_c does not exceed ~ 0.75 K [3, 11]. However in CeAg₂Si₂, optimal SC with $T_c = 1.25$ K occurs roughly 3 GPa above the magnetic p_c , and partial SC persists up to ~ 21 GPa, i.e, roughly 8 GPa above p_c .

(iii) From a larger point of view, the magnetic phase diagram is different for each compound of the CeCu₂Si₂-HF family, while all other properties including SC are quite similar [9, 10, 15, 16, 18, 19].

In summary, we have discovered HF SC in CeAg₂Si₂ and established its the p - T phase diagram up to 22.5 GPa. The magnetic phase, whose transition line first increases with increasing pressure, suddenly collapses at $p_c \sim 13$ GPa. SC emerges close to p_c , is optimal with $T_c = 1.25$ K at $p \sim 16$ GPa, and persist over a huge pressure range of roughly 10 GPa. Several features in the resistivity strongly suggest a pressure-induced VCO in proximity to optimal SC. The crossover arises from a putative valence transition CEP at critical pressure $p_{\text{cr}} \sim 17$ GPa and temperature $T_{\text{cr}} \sim -13$ K. In particular, the isotherms of the normalized resistivity plotted versus the generalized distance from the CEP collapse on a single scaling function. From these findings we emphasize that, besides spin fluctuations, valence fluctuations are a key ingredient in the low-temperature physics of CeAg₂Si₂. New experiments with better resolution on the pressure scale will be essential to clarify the exact nature of the phase transition at p_c and of the SC pairing mechanism.

V. ACKNOWLEDGMENTS

We acknowledge enlightening discussions with Shinji Watanabe and Kazumasa Miyake and technical support from Marco Lopez and Sebastian Müller.

-
- [1] K. Miyake, S. Schmitt-Rink, and C. M. Varma, Phys. Rev. B **34**, 6554 (1986).
 - [2] D. J. Scalapino, E. Loh, Jr., and J. E. Hirsch, Phys. Rev. B **34**, 8190(R) (1986).
 - [3] N. D. Mathur, F. M. Grosche, S. R. Julian, I. R. Walker, D. M. Freye, R. K. W. Haselwimmer, and G. G. Lonzarich, Nature **394**, 39 (1998).
 - [4] P. Monthoux, D. Pines, and G. G. Lonzarich, Nature **450**, 1177 (2007).
 - [5] K. Miyake, J. Phys.: Condens. Matter **19**, 125201 (2007).
 - [6] O. Stockert, J. Arndt, E. Faulhaber, C. Geibel, H. S. Jeevan, S. Kirchner, M. Loewenhaupt, K. Schmalzl, W. Schmidt, Q. Si, and F. Steglich, Nat. Phys. **7**, 119 (2011).
 - [7] F. Steglich, J. Aarts, C. D. Bredl, W. Lieke, D. Meschede, W. Franz, and H. Schäfer, Phys. Rev. B **43**, 1892 (1979).
 - [8] B. Bellarbi, A. Benoit, D. Jaccard, J. M. Mignot, and H. F. Braun, Phys. Rev. B **30**, 1182 (1984).

- [9] A. T. Holmes, D. Jaccard, and K. Miyake, *Phys. Rev. B* **69**, 024508 (2004).
- [10] D. Jaccard, H. Wilhelm, K. Alami-Yadri, and E. Vargoz, *Physica B* **259-261**, 1 (1999).
- [11] H. Q. Yuan, F. M. Grosche, M. Deppe, C. Geibel, G. Sparn, and F. Steglich, *Science* **302**, 2104 (2003).
- [12] J. Arndt, O. Stockert, K. Schmalzl, E. Faulhaber, H. S. Jeevan, C. Geibel, W. Schmidt, M. Loewenhaupt, and F. Steglich, *Phys. Rev. Lett.* **106**, 246401 (2011).
- [13] A. T. Holmes, D. Jaccard, and K. Miyake, *J. Phys. Soc. Jpn.* **76**, 051002 (2007).
- [14] S. Watanabe and K. Miyake, *J. Phys.: Condens. Matter* **23**, 094217 (2011).
- [15] G. Seyfarth, A. S. Rüetschi, K. Sengupta, A. Georges, D. Jaccard, S. Watanabe, and K. Miyake, *Phys. Rev. B* **85**, 205105 (2012).
- [16] Z. Ren, L. V. Pourovskii, G. Girit, G. Lapertot, A. Georges, and D. Jaccard, *Phys. Rev. X* **4**, 031055 (2014).
- [17] Z. Ren, G. Girit, G. W. Scheerer, G. Lapertot, and D. Jaccard, *Phys. Rev. B* **91** 094515 (2015).
- [18] Z. Ren, G. W. Scheerer, G. Lapertot, and D. Jaccard, *Phys. Rev. B* **94**, 024522 (2016).
- [19] G. W. Scheerer, G. Girit, Z. Ren, G. Lapertot, and D. Jaccard, *J. Phys. Soc. Jpn.* **86**, 064710 (2017).
- [20] B. H. Grier, J. M. Lawrence, V. Murgai, and R. D. Parks, *Phys. Rev. B* **29**, 2664 (1984).
- [21] A. Severing, E. Holland-Moritz, B. D. Rainford, S. R. Culverhouse, and B. Prick, *Phys. Rev. B* **39**, 2557 (1989).
- [22] C. S. Garde and J. Ray, *J. Phys.: Condens. Matter* **6**, 8585 (1994).
- [23] V. Murgai, S. Raaen, L. C. Gupta, and R. D. Parks, *Valence Instabilities* P. 537 (North-Holland, Amsterdam, 1982).
- [24] J. D. Thompson, R. D. Parks and H. Borges, *J. Magn. Magn. Mater.* **54**, 377 (1986).
- [25] T. T. M. Palstra, A. A. Menovsky, G. J. Nieuwenhuys and J. A. Mydosh, *J. Magn. Magn. Mater.* **54**, 435 (1986).
- [26] P. Link, D. Jaccard, and P. Lejay, *Physica B* **225**, 207 (1996).
- [27] Z. Mo and B. H. Grier, *J. Phys.: Condens. Matter* **1**, 4947 (1989).
- [28] B. Corbut and B. Coqblin, *Phys. Rev. B* **5** 4541 (1972).
- [29] D. Jaccard, J. M. Mignot, B. Bellarbi, A. Benoit, H. F. Braun, and J. Sierro, *J. Magn. Magn. Mater.* **47-48**, 23 (1985).
- [30] H. Wilhelm, S. Raymond, D. Jaccard, O. Stockert, and H. v. Loehneysen, *Science and technology of high pressure*, Proc. of AIRAPT-17, ed. M. H. Manghnani. (Universities Press India, Hyderabad, 2000), p. 697.
- [31] H. Wilhelm and D. Jaccard, *Phys. Rev. B* **66**, 064428 (2002).
- [32] A. Demuer, A.T.Holmes, and D. Jaccard, *J. Phys.: Condens. Matter* **14**, L529 (2002).
- [33] $\rho(T)$ data of CeRhIn₅ under hydrostatic pressure up to 5.6 GPa, Ren *et al.*, in preparation.
- [34] Y. Nishida, A. Tsuruta, and K. Miyake, *J. Phys. Soc. Jpn.* **75**, 064706 (2006).
- [35] In general, the $\rho = 0$ criteria coincides with signatures of bulk SC in calorimetry or magnetic susceptibility signals ([15, 16, 19] and [G. Girit, Z. Ren, P. Pedrazzini, and D. Jaccard, *Solid State Commun.* **209-210**, 55 (2015)]).
- [36] T. P. Orlando, E. J. McNiff, Jr., S. Foner, and M. R. Beasley, *Phys. Rev. B* **19**, 4545 (1979).
- [37] K. Miyake and O. Narikiyo, *J. Phys. Soc. Jpn.* **71**, 867 (2002).
- [38] K. Hattori and K. Miyake, *J. Phys. Soc. Jpn.* **79**, 073702 (2010).
- [39] K. Miyake and H. Maebashi, *J. Phys. Soc. Jpn.* **71**, 1007 (2002).
- [40] J. Flouquet, Y. Haga, P. Haen, D. Braithwaite, G. Knebel, S. Raymond, and S. Kambe, *J. Magn. Magn. Mater.* **272**, 27 (2004).
- [41] E. Vargoz, D. Jaccard, J.-Y. Genoud, J.-P. Brison, and J. Flouquet, *Solid State Commun.* **106**, 631 (1998).
- [42] G. Knebel, C. Eggert, D. Engelmann, R. Viana, A. Krimmel, M. Dressel, and A. Loidl, *Phys. Rev. B* **53**, 11586 (1996).
- [43] E. Vargoz, Dr. thesis, DPMC, Université de Genève, Geneva (1998).
- [44] Y. Onishi and K. Miyake, *J. Phys. Soc. Jpn.* **69**, 3955 (2000).
- [45] S. Watanabe, M. Imada, and K. Miyake, *J. Phys. Soc. Jpn.* **75**, 043710 (2006).
- [46] A. Okada and K. Miyake, *J. Phys. Soc. Jpn.* **80**, 084708 (2011).
- [47] S. Watanabe and K. Miyake, *J. Phys. Soc. Jpn.* **79**, 033707 (2010).